Accurate Centerline Detection and Line Width Estimation of Thick Lines Using the Radon Transform

Article *in* IEEE Transactions on Image Processing · March 2007

DOI: 10.1109/TIP.2006.887731 · Source: PubMed

2 authors:

Qiaoping Zhang
Intermap Technologies Corp.
34 PUBLICATIONS **279** CITATIONS

SEE PROFILE

Isabelle Couloigner
The University of Calgary
37 PUBLICATIONS **454** CITATIONS

SEE PROFILE

Accurate Centerline Detection and Line Width Estimation of Thick Lines Using the Radon Transform

Qiaoping Zhang and Isabelle Couloigner

***Abstract*—Centerline detection and line width estimation are important for many computer vision applications, e.g., road network extraction from high resolution remotely sensed imagery. Radon transform-based linear feature detection has many advantages over other approaches: for example, its robustness in noisy images. However, it usually fails to detect the centerline of a thick line due to the peak selection problem. In this paper, several key issues that affect the centerline detection using the radon transform are investigated. A mean filter is proposed to locate the true peak in the radon image and a profile analysis technique is used to further refine the line parameters. The θ-boundary problem of the radon transform is also discussed and the erroneous line parameters are corrected. Intensive experiments have shown that the proposed methodology is effective in finding the centerline and estimating the line width of thick lines.**

***Index Terms*—Image line pattern analysis, object detection, radon transforms, remote sensing.**

I. Introduction

THE RADON transform is able to transform images with lines into a domain of possible line parameters, where each line in the image will give a peak (for a bright line) or a valley (for dark line) positioned at the corresponding line parameters. This has led to many line detection applications within image processing, computer vision, and seismic applications [1]. The radon transform-based linear feature detector is less sensitive to the noise in the image than other linear feature detectors because the intensity fluctuations due to noise tend to be cancelled out by the process of integration [2]. Therefore, in remote sensing, it has been widely used in linear feature (e.g., ship wakes) detection on Synthetic Aperture Radar (SAR) images [2]–[5].

However, the radon transform-based linear feature detector has some issues. First, it fails to provide an indication of the line length or the end-point positions, and cannot be relied upon to detect linear features of short extent [2]. Second, linear features that span the entire image but display some curvature may not produce suitable peaks (or valleys) in the transform domain [3]. Third, locating the peaks is very difficult in some cases, and, thus, an accurate estimation of the line parameters is not straightforward. Finally, it does not accurately locate the centerline of thick lines but locates their diagonals instead [6]. The last two issues are associated with the peak selection of the radon transform.

In the last two decades, substantial work has been completed to improve the quality of the radon transform-based linear feature detectors. In [3], Copeland *et al.* modified the radon transform so as to localize the area in which each integration takes place. This reduces the problem of integrating through more noise than necessary, which tends to obscure the peak (or valley) corresponding to a linear feature that is much shorter than the image dimensions. It can also produce better results if the linear features display some curvature. Unfortunately, the localization of the radon transform prevents us from using the popular frequency domain calculation method [2] to save computation time.

In their auto-extraction of linear features, such as guard-rails from vehicle-borne laser data, Manandhar and Shibasaki [7] used a Circle Growing algorithm to find the end points of the linear features based on a radon transform. Morphological operations were used to select the peaks from the radon image, which involved dilation using structuring line elements and threshold values of the radon space. However, thresholding after a morphological operation like dilation does not solve the peak selection problem since the original radon peak is often biased.

Based on the gliding-box algorithm and the radon transform algorithm, a novel method for detecting ship wakes in SAR images is proposed in [4]. This method is applied to both simulated and real SAR images. The result shows that the detection accuracy is satisfactory in a strong noise environment. One significant feature of the new algorithm is that it can even detect ship wakes, which are significantly shorter than the image dimensions.

To avoid wide lines causing varying problems during detection, Clode *et al.* [6] convolve a raw, pixelated, binary road classification with a complex-valued disk. This technique provides three separate pieces of information about the road or thick line: the centerline, the direction, and the width of the road at any point along the centerline. The road centerline can be detected from the position of the magnitude peak in the magnitude image resulting from the complex convolution. Road width can also be estimated from the magnitude peak while the direction may be obtained from the phase image. Tests on Lidar data have shown that the proposed methodology was able to detect thick curvilinear lines. However, the technique failed to give proper results on a road intersection and it was difficult to determine the road width.

Manuscript received July 4, 2005 ; revised July 4, 2006. This work was supported in part by the Canadian NCE GEOIDE research program "Automating photogrammetric processing and data fusion of very high resolution satellite imagery with LIDAR, iFSAR and maps for fast, low-cost and precise 3D urban mapping." The associate editor coordinating the review of this manuscript and approving it for publication was Dr. Jacques Blanc-Talon.

Q. Zhang was with the Department of Geomatics Engineering, University of Calgary, Calgary, AB T2N 1N4 Canada. He is now with Intermap Technologies Corporation, Calgary, AB T2P 3E7 Canada (e-mail: qzhang@intermap.com).

I. Couloigner is with the Department of Geomatics Engineering, University of Calgary, Calgary, AB T2N 1N4 Canada (e-mail: couloigner@geomatics.ucalgary.ca).

Color versions of one or more of the figures in this paper are available online at http://ieeexplore.ieee.org.

Digital Object Identifier 10.1109/TIP.2006.887731

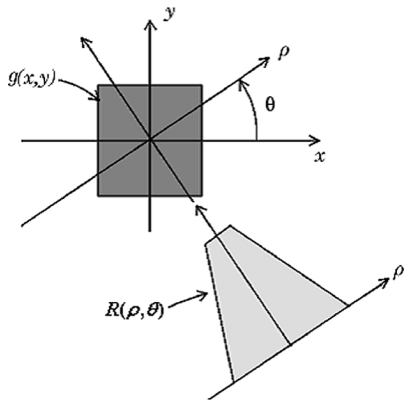

Fig. 1. Geometry of the radon transform (after [8]).

Theoretically, it is very simple to detect a line in an image based on the radon transform. However, in practice, there are many cases for which we do not get accurate results or the line detection fails. In this paper, we are focusing on the peak selection problem to find the centerlines of thick lines based on the radon transform. It is an important issue for different applications such as road network extraction on high resolution remotely sensed imagery. The remaining sections of this paper are organized as follows. The basic radon transform is described in Section II. Then, the issues of line detection using the radon transform is discussed in Section III followed by an introduction to the line width estimation techniques in Section IV. Section V gives the test data and the experimental results. We summarize our research and conclude the paper in Section VI.

II. Basic Radon Transform

The radon transform of a function $g(x,y)$ in 2-D Euclidean space is defined by [2]

$$R(\rho,\theta)=\int_{-\infty}^{\infty}\int_{-\infty}^{\infty}g(x,y)\delta(\rho-x\cos\theta-y\sin\theta)dxdy$$

where the $\delta(r)$ is the Dirac function which is infinite for argument zero and zero for all other arguments (it integrates to one). The presence of the term $\delta(\rho-x\cos\theta-y\sin\theta)$ in the definition of the radon transform forces the integration of $g(x,y)$ along the line defined by

$$\rho-x\cos\theta-y\sin\theta=0.$$

Consequently, if $g(x,y)$ is a 2-D image intensity function, computation of its radon transform yields the projections across the image at varying orientations θ and offsets ρ (relative to a parallel line passing through the image center) [2]. The radon transform should, therefore, contain a peak corresponding to every line in the image that is brighter than its surroundings and a valley for every dark line. Thus, the problem of detecting lines is reduced to detecting the peaks and valleys in the transform domain [3]. The geometry of the radon transform is illustrated in Fig. 1.

III. Line Parameter Estimation in the Radon Transform

In general, lines are detected by using the parameters (ρ, θ) derived from the peaks (or valleys) in the radon space. However, complications may occur when the peaks (or valleys) are ambiguous or biased along either the offset (ρ) or the orientation (θ), or both. In addition, there is a θ-boundary problem because the radon transform is usually calculated based on a limited range of direction angles.

All the test images used in this paper are assumed to have bright lines on a dark background. Therefore, only the peaks in the radon space are of concern. However, for illustration purpose, we are showing the inverse of all the input images in the following figures. The step size of θ in the radon transform is set to 1° for all the cases.

A. Biased Radon Peak: One Direction

Fig. 2 is an example of a biased peak along the ρ direction. In Fig. 2(a), the black line is about five pixels in width. The dashed line is reconstructed from the parameters determined by the original radon peak. As we can see from the figure, the detected line is shifted away from the actual centerline. This is because the peak in the radon domain is not a simple unique point but a small peak region [Fig. 2(b)] and the ρ value that forms the peak radon value is biased along the profile in the ρ direction [Fig. 2(c)].

To obtain a better estimation of the ρ value of the line, a profile analysis technique is used. A profile along the ρ direction passing the peak is plotted [Fig. 2(c)]. Two values, ρ_1 and ρ_2, are determined by using a linear interpolation based on a semi-peak radon value, which is 90% of the peak radon value [Fig. 2(c)]. The determination of the semi-peak radon value is based on our observation that the difference between the biased radon peak value and the true radon peak value is usually less than 10%. 90% is selected so that the true radon peak is included in the range while keeping the range as small as possible. In fact, decreasing the number (e.g., to 75%) will not significantly affect the final result if the radon peak region is close to symmetric in the θ direction. However, increasing the number (e.g., to 95%) will risk losing the true radon peak in the range. The ρ value of the line is then determined by the average of these two values, i.e.

$$\hat{\rho}_0=\frac{(\rho_1+\rho_2)}{2}.$$

Similar steps are used for an accurate estimation of the θ value

$$\hat{\theta}_0=\frac{(\theta_1+\theta_2)}{2}.$$

The reconstructed line with the new estimated parameters ($\hat{\rho}_0$, $\hat{\theta}_0$) is shown in Fig. 2(d). It is clear that the proposed method gives a more accurate estimation of the line parameters than using the original radon peak. The new reconstructed line coincides accurately with the actual centerline of the wide line.

Fig. 3 illustrates two other results from our simulated images. The problem with these two images is that the radon peaks are biased along the θ direction [Fig. 3(a) and (c)]. It is evident that the proposed approach corrects one of the problems with the radon transform-based line detection. The exact centerline of the

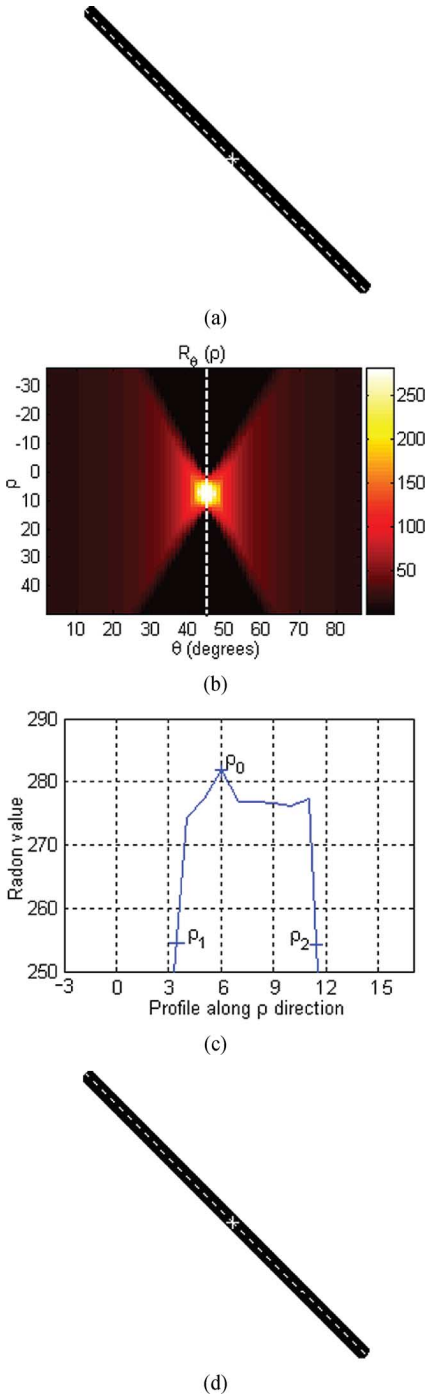

Fig. 2. Accurate line parameter estimation in the radon transform using the profile analysis technique: (a) the input image and the reconstructed line (dashed) based on the original radon peak; (b) the radon transform; (c) a profile along the ρ direction shown as a white dashed line in (b) and an illustration of the estimation of the ρ value; (d) the reconstructed line using the refined radon peak.

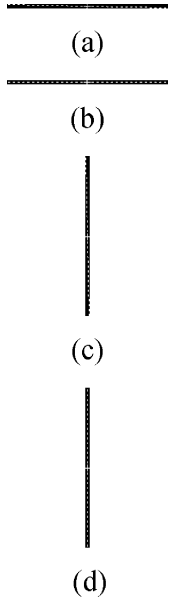

Fig. 3. Examples of accurate line parameter estimation in the radon transform [(a)–(d): shrunken version, original image size is 200 × 200 with the line under consideration in the center]: (a) and (c) show the reconstructed line (dashed) using the original radon peak; (b) and (d) show the reconstructed line (dashed) using the refined radon peak.

thick lines [Fig. 3(b) and (d)] is detected instead of the diagonal line, which is the case when the original radon peak is used.

B. Biased Radon Peak: Both Directions

The profile analysis technique, however, does not work if the radon peak is biased in both ρ and θ directions because, in this case, the true line parameters are no longer on the profiles passing the peak. Fig. 4 illustrates this problem. The radon transform of the input image [Fig. 4(a)] is shown in Fig. 4(c) with its zoomed version in Fig. 4(d). The reconstructed centerline based on the original radon peak is shown as a white dashed line in Fig. 4(a). It is clear that the centerline is not accurate. Numerically, the radon peak is at R_0 (84.0°, 93.0°). The refined radon peak using the profile analysis approach is at (84.1°, 92.8°). It is not yet accurate enough although it is closer to the true position R_1 (88.0°, 90.0°).

A low-pass filter applied to the radon image will remove the undesirable variations of radon peak values in the radon image and help us find the true radon peak. The low-pass filter can be a mean filter, a Gaussian filter, or a median filter. The simplest mean filter was chosen for use in this paper. The element with the highest mean radon value within the filter window is selected as the peak and is used to estimate the line parameters [Fig. 4(d)]. The choice of the filter size is mainly based on the average thickness of the lines. Experiments show that the filter size should be less than but close to the average thickness of the lines. For example, 3 × 3 is used for an average width of 5 pixels and 7 × 7 for an average width of 10 pixels. The filter size used in this example is 3 × 3. The improved result is shown in Fig. 4(b).

C. θ-Boundary Problem

The θ-boundary problem of the radon transform is associated with a vertical line. The peak region corresponding to the vertical line is artificially divided into two discontinuous parts in the radon transform because the θ used is between 0° and 180°. The true radon peak corresponding to the true line parameters is located exactly on the boundary ($\theta = 180°$). Both the profile analysis and the mean-filter methods fail to find the true radon peak because of the θ-boundary problem. Fig. 5 illustrates this

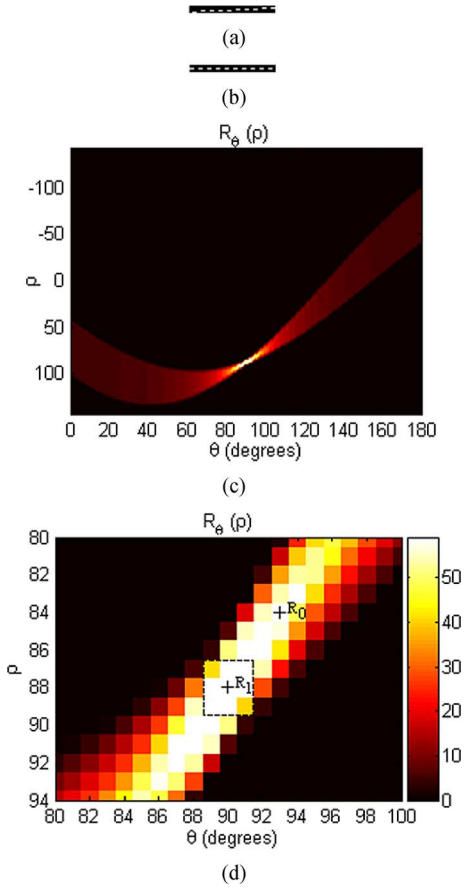

Fig. 4. Accurate line parameter estimation in the radon transform using a mean filter [(a)–(d): shrunken version, original image size is 200 × 200 with the line under consideration in the center]: (a) the input image and the reconstructed centerline (dashed) based on the original radon peak; (b) the reconstructed line (dashed) using the refined line parameters based on the radon peak found by a mean filter; (c) the radon transform; (d) zoom in version of (c). R_0: the original radon peak; R_1: the radon peak found by the mean filter, the black dashed line shows the window used.

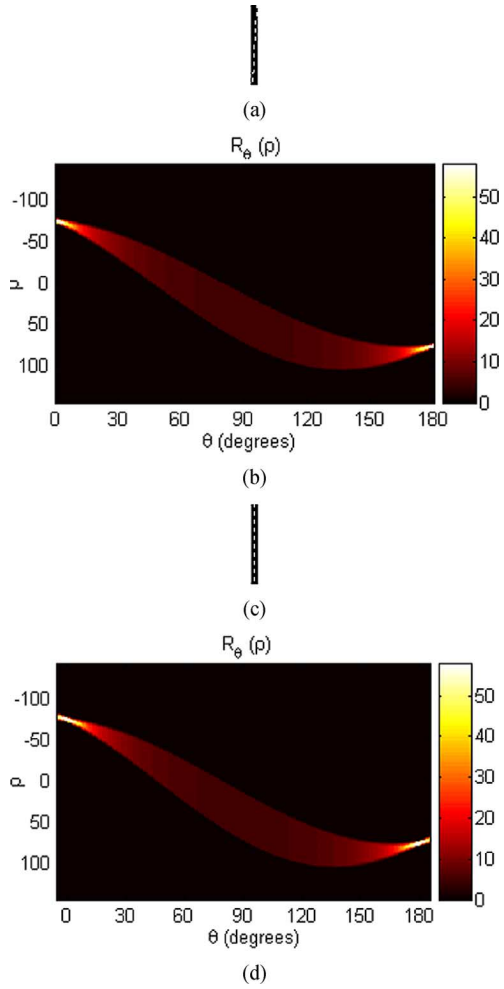

Fig. 5. Example of θ-boundary problem of the radon transform [(a) and (c): shrunken version, original image size is 200 × 200 with the line under consideration in the center]: (a) input image with the reconstructed line (dashed) based on the original radon peak; (b) the radon transform; (c) the new reconstructed line (dashed) using the refined line parameters; (d) the expanded radon transform with θ as $[-5°, 185°]$.

problem. The radon transform of the input image [Fig. 5(a)] is shown in Fig. 5(b), where the θ-boundary problem is evident. The solution is to use θ from $-5°$ to 185° in the radon transform to allow an overlapping area along the θ direction [Fig. 5(d)]. The final result is shown in Fig. 5(c).

IV. Line Width Estimation in the Radon Transform

The estimation of the line width is important for many linear feature detection applications such as road network extraction from remotely sensed imagery for the purpose of updating a digital road database. Different road widths often indicate different road classes. However, most road detectors fail to give an accurate and robust estimation of road widths. A dynamic programming approach (e.g., [9]) does not give any information of line width. In a template matching approach (e.g., [10]), line width is preset usually with a limited adjustability during the matching process. Line width estimated from a profile analysis technique (e.g., [11] and [12]) or from a morphological thinning-based approach (e.g., [13]) is usually sensitive to the noisy pixels. These techniques, thus, fail to give a meaningful line width for a real road. With a radon transform-based linear feature detector, we can estimate the line width for each detected line segment.

The width ($W\rho$) in the ρ direction of a peak in a radon transform provides an estimate of the mean width of the corresponding linear feature [2]. The only problem is in the determination of $W\rho$. In this research, two ρ values, ρ'_1 and ρ'_2, are determined based on the half-peak radon value, which is 50% of the peak radon value. The half-peak radon value is used in the mean line width calculation because any pixel contributing to the half-peak radon value during the radon integration should be taken into consideration in the line width calculation. The width $W\rho$ is then calculated using the following equation:

$$W_\rho = \rho'_2 - \rho'_1.$$

The results from a number of test images are summarized in Table I. The real line widths are calculated based on the geometric relationship illustrated in Fig. 6 and the following equation:

$$\frac{w}{a} = \frac{b}{c} = \frac{b}{\sqrt{a^2+b^2}} \Rightarrow w = \frac{ab}{\sqrt{a^2+b^2}}.$$

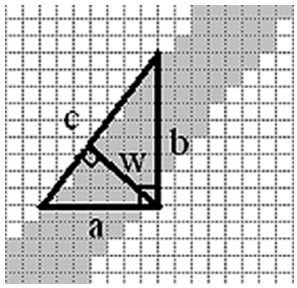

Fig. 6. Calculation of line width.

TABLE I
LINE WIDTH ESTIMATION (IN PIXELS)

Line No	"Real" value	Estimated	Error
1	4.2	4.5	-0.3
2	9.9	9.5	0.4
3	9.9	9.5	0.4
4	5.0	4.8	0.2
5	5.0	4.8	0.2
6	5.0	4.8	0.2
7	5.0	4.8	0.2
8	5.0	4.7	0.3
9	5.0	4.9	0.1
10	5.0	4.7	0.3
11	5.0	4.9	0.1
12	5.0	4.9	0.1
13	5.0	4.9	0.1
14	3.0	3.0	0.0
15	4.2	4.0	0.2
16	4.2	4.0	0.2
17	4.2	4.4	-0.2
18	4.3	4.6	-0.3
19	4.2	4.3	-0.1
20	4.2	4.3	-0.1
		Mean	0.1
		RMSE	± 0.20

The "real" values of a and b are manually measured on the input images once the images are zoomed in enough to ensure measurement accuracy. It is clear that the proposed approach is capable of estimating an accurate line width based on the radon transform. The mean of the errors is $+0.1$ pixels and the root mean-square error (RMSE) is approximately ± 0.2 pixels, which is accurate enough for most applications.

V. EXPERIMENTS

The proposed radon transform method has been tested on numerous images.

A. Synthetic Image

A typical result from one of our simulated images is illustrated in Fig. 7. Fig. 7(a) shows the reconstructed centerlines based on the original radon peaks. Fig. 7(b) presents the results from our proposed approach. It can be clearly seen from lines 1, 4, and 6 that the results from our method are more accurate than those from the original method. The estimated line widths are shown in Table II. The mean error is only 0.1 pixels.

Results from Fig. 8 indicate that the applicability of the proposed approach to centerline detection of thick lines is quite encouraging. The six line widths are approximately 10 pixels. The improvements are evident when comparing Fig. 8(b) with Fig. 8(a). The estimated line widths (Table III) are also very accurate. This indicates that the proposed method is not sensitive to the width of the lines.

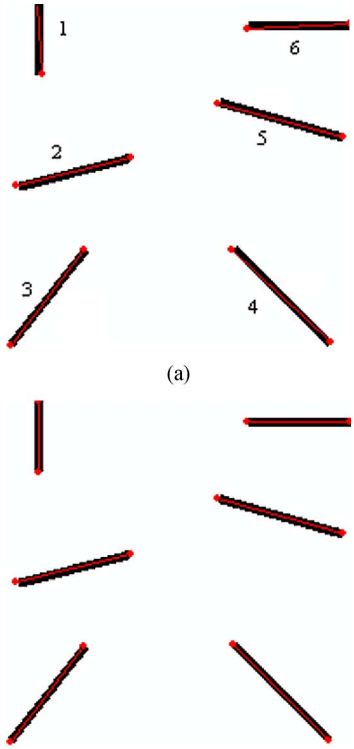

Fig. 7. Centerline detection using the radon transform: (a) the reconstructed lines (red) based on the original radon peaks; (b) the improved results.

TABLE II
LINE WIDTH ESTIMATION (IN PIXELS)

Line No	"Real" value	No noise		With noise	
		Estimated	Error	Estimated	Error
1	5.0	5.0	0.0	5.1	-0.1
2	5.0	5.1	-0.1	5.3	-0.3
3	4.6	4.7	-0.1	4.8	-0.2
4	4.2	4.3	-0.1	4.4	-0.2
5	5.0	5.1	-0.1	5.2	-0.2
6	5.0	5.0	0.0	5.1	-0.1
		Mean	-0.1		-0.2
		RMSE	± 0.05		± 0.07

B. Synthetic Image With Noise

To test the robustness of the proposed method, we added a salt and pepper noise with a 0.05 noise density to the original images. The outputs are shown in Figs. 9 and 10. The estimated line widths are listed in Tables II and III, respectively. The extracted centerlines from the noisy images are a little bit less accurate than that from the images free of noise, but are well within acceptable quality. This confirms that the proposed method is able to accurately extract the centerlines in a noisy image together with a precise estimation of the line widths.

C. Real Classified Satellite Image

The proposed radon transform has also been applied to a set of classified images. The input images are IKONOS multispectral images with a 4-m spatial resolution. A traditional spectral

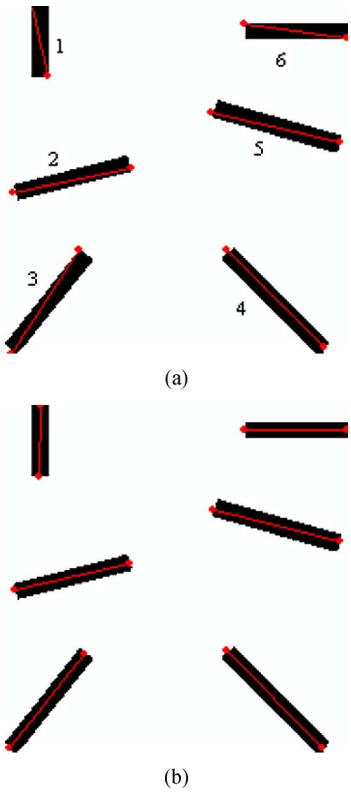

Fig. 8. Centerline detection of thick lines using the radon transform: (a) the reconstructed lines (red) based on the original radon peaks; (b) the improved results.

clustering, a fuzzy logic classification and a road pixel refinement have been applied to the input images to create binary road network images. The road pixel refinement aimed to remove the spectrally similar objects (e.g., parking lots, buildings, crop fields) from the road class. It was achieved by using a set of shape descriptors of the Angular Texture Signature. Details can be found in [14]. The improved radon transform are then applied to the refined road pixels to extract the road centerlines. Figs. 11 and 12 illustrate some of the results of the road centerline extraction. The multiple road lines present on the images were detected by applying the radon transform iteratively. At each iteration only one road line was detected from the current radon peak. The road pixel image was then updated by removing the road pixels corresponding to the detected road line. The iteration ended when there was no more road line to detect. Because there is no ground truth available for evaluation purpose, we manually calculated the road widths on the 1-m spatial resolution panchromatic image. The calculated road widths were then used as a reference to evaluate the road width estimation by the improved radon transform. The evaluation result (Table IV) shows that the estimated road widths are generally overestimated. This is because the input image has lower spatial resolution than the reference one, thus more pixel mixing. However, from Figs. 11 and 12, we can see that the proposed methodology is able to detect road segments on classified imagery with a good estimation of road width and with a good positional accuracy.

TABLE III
LINE WIDTH ESTIMATION (IN PIXELS)

Line No	"Real" value	No noise		With noise	
		Estimated	Error	Estimated	Error
1	10.0	10.0	0.0	10.2	-0.2
2	9.7	9.4	0.3	9.6	0.1
3	10.1	9.8	0.3	9.8	0.3
4	9.9	9.9	0.0	10.0	-0.1
5	10.6	10.5	0.1	10.5	0.1
6	9.0	9.0	0.0	9.2	-0.2
		Mean	0.1		0.0
		RMSE	± 0.13		± 0.18

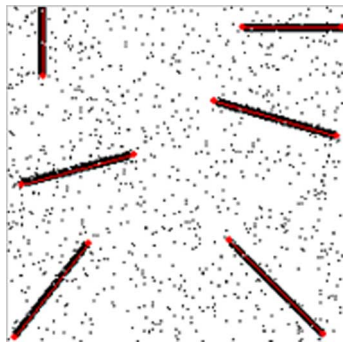

Fig. 9. Detected centerline (red) from the degraded input image in Fig. 7.

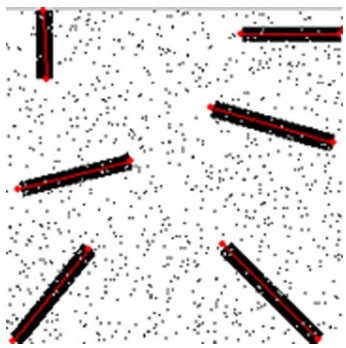

Fig. 10. Detected centerline (red) from the degraded input image in Fig. 8.

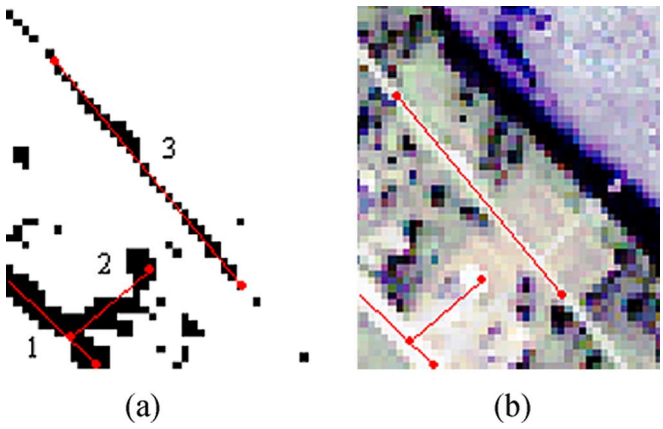

Fig. 11. Detected road centerlines (red) overlaid on (a) the road pixels and (b) the IKONOS MS true composite image. The estimated line widths for lines 1–3 are 3.3, 3.9, and 2.0 pixels, respectively.

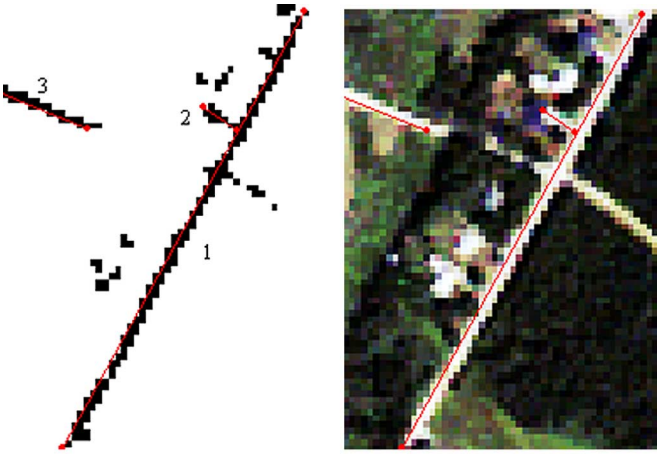

Fig. 12. Detected road centerlines (red) overlaid on (a) the road pixels and (b) the IKONOS MS true composite image. The estimated line widths for lines 1–3 are 2.4, 2.3, and 2.2 pixels, respectively.

TABLE IV
LINE WIDTH ESTIMATION (IN PIXELS)

Line		Fig.11			Fig.12	
No	"Real"	Estimated	Error	"Real"	Estimated	Error
1	3.1	3.3	-0.2	2.3	2.4	-0.1
2	3.6	3.9	-0.3	2.1	2.3	-0.2
3	1.5	2.0	-0.5	2.0	2.2	-0.2
		Mean	-0.4			-0.2
		RMSE	± 0.12			± 0.05

VI. CONCLUSION

The radon transform has a number of advantages for linear feature detection including its ability to detect line width and its robustness to noise, the quality of the radon transform-based linear feature detector has to be improved for some applications such as road network extraction from remotely sensed imagery. In this paper, the peak selection problem in the radon transform-based line detector is investigated. A mean filter is proposed to locate the true peak in the radon image and a profile analysis technique is used to further refine the line parameters. The θ-boundary problem of the radon transform is also discussed and the erroneous line parameters are corrected. Experiments have shown that the proposed methodology gives an accurate and robust estimation of the line parameters. It provides a solution to the peak selection issue of the radon transform-based linear feature detector.

Other issues relating to the application of the radon transform to linear feature detection on large images where it is difficult to detect the lines of short extent, the centerline detection and line width estimation of curvilinear lines, and the quantitative evaluation of the extracted centerlines will be included in our future work.

ACKNOWLEDGMENT

The authors would like to thank the City of Fredericton, NB, Canada, for providing the satellite images.

REFERENCES

[1] P. Toft, "The Radon Transform—Theory and Implementation," Ph.D. dissertation, Dept. Math. Model., Tech. Univ. Denmark, Lyngby, 1996.
[2] L. M. Murphy, "Linear feature detection and enhancement in noisy images via the Radon transform," *Pattern Recognit. Lett.*, vol. 4, pp. 279–284, 1986.
[3] A. C. Copeland, G. Ravichandran, and M. M. Trivedi, "Localized Radon transform-based detection of ship wakes in SAR images," *IEEE Trans Geosci. Remote Sens.*, vol. 33, no. 1, pp. 35–45, Jan. 1995.
[4] G. Du and T. S. Yeo, "A novel Radon transform-based method for ship wake detection," in *Proc. IEEE Int. Conf. Geoscience and Remote Sensing Symp.*, Anchorage, AK, Sep. 20–24, 2004, pp. 3069–3072.
[5] G. Zilman, A. Zapolski, and M. Marom, "The speed and beam of a ship from its wake's SAR images," *IEEE Trans Geosci. Remote Sens.* , vol. 42, no. 10, pp. 2335–2343, Oct. 2004.
[6] S. P. Clode, E. E. Zelniker, P. J. Kootsookos, and I. V. L. Clarkson, "A phase coded disk approach to thick curvilinear line detection," in *Proc. 7th Eur. Signal Processing Conf.*, Vienna, Austria, Sep. 6–10, 2004, pp. 1147–1150.
[7] D. Manandhar and R. Shibasaki, "Extraction of linear features from vehicle-borne laser data," presented at the 23rd Asian Conf. Remote Sensing, Kathmandu, Nepal, Nov. 25–29, 2002.
[8] *Radon Transform, Image Processing Toolbox User's Guide, Matlab Help Document*. Natick, MA: MathWorks, Inc., 2005.
[9] A. Gruen and H. Li, "Semi-automatic linear feature extraction by dynamic programming and LSB-snakes," *Photogramm. Eng. Remote Sens.*, vol. 63, no. 8, pp. 985–995, 1997.
[10] X. Hu, Z. Zhang, and C. V. Tao, "A robust method for semi-automatic extraction of road centerlines using a piecewise parabolic model and least square template matching," *Photogramm. Eng. Remote Sens.*, vol. 70, no. 12, pp. 1393–1398, Dec. 2004.
[11] J. Wang and Q. Zhang, "Applicability of a gradient profile algorithm for road network extraction-sensor, resolution and background considerations," *Canad. J. Remote Sens.*, vol. 26, no. 5, pp. 428–439, 2000.
[12] X. Hu and C. Tao, "A reliable and fast ribbon road detector using profile analysis and model-based verification," *Int. J. Remote Sens.*, vol. 26, no. 5, pp. 887–902, 2005.
[13] M. Song and D. Civco, "Road extraction using SVM and image segmentation," *Photogramm. Eng. Remote Sens.*, vol. 70, no. 12, pp. 1365–1371, Dec. 2004.
[14] Q. Zhang and I. Couloigner, "Benefit of the angular texture signature for the separation of parking lots and roads on high resolution multi-spectral imagery," *Pattern Recognit. Lett.*, vol. 27, no. 9, pp. 937–946, 2006.

Qiaoping Zhang was born in Dongyang, China, in 1971. He received the B.Sc. and a M.Sc. degrees in surveying engineering from Hohai University, Nanjing, China, in 1993 and 1996 respectively, the Ph.D. degree in photogrammetry and remote sensing from Wuhan University, Wuhan, China in 2002, and the Ph.D. degree in geomatics engineering from the University of Calgary, Calgary, AB, Canada in 2006.

He was a Lecturer in the Department of Surveying Engineering, Hohai University, China, from 1993 to 1998. His research interests include object extraction from remotely sensed imagery for change detection and geographical database updating.

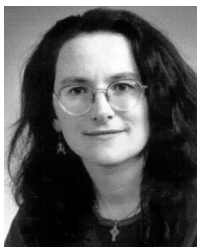

Isabelle Couloigner was born in Brest, France, in 1969. She received the engineering diploma in electronics (detection and telecommunications) from the French Engineering School, Ecole Louis de Broglie, Rennes, France, in 1994. She did her Ph.D. studies at the French Engineering School, Ecole des Mines de Paris, Paris, France, and received the Ph.D. degree in sciences for engineer (propagation, telecommunications, and remote sensing) from the Université de Nice-Sophia Antipolis, France, in 1998.

She was a Postdoctoral Fellow at the Centre de Recherche en Géomatique, Université Laval, Laval, QC, Canada, from 1999 to 2000. She has been an Assistant Professor with the Department of Geomatics Engineering, University of Calgary, Calgary, AB, Canada, since January 2001. Her research mainly focuses on the application of data fusion (remote-sensing imagery, topographic database, GIS, and ancillary data) and wavelet transforms to feature modeling and extraction from high spatial resolution imagery.